Supplemental Figures

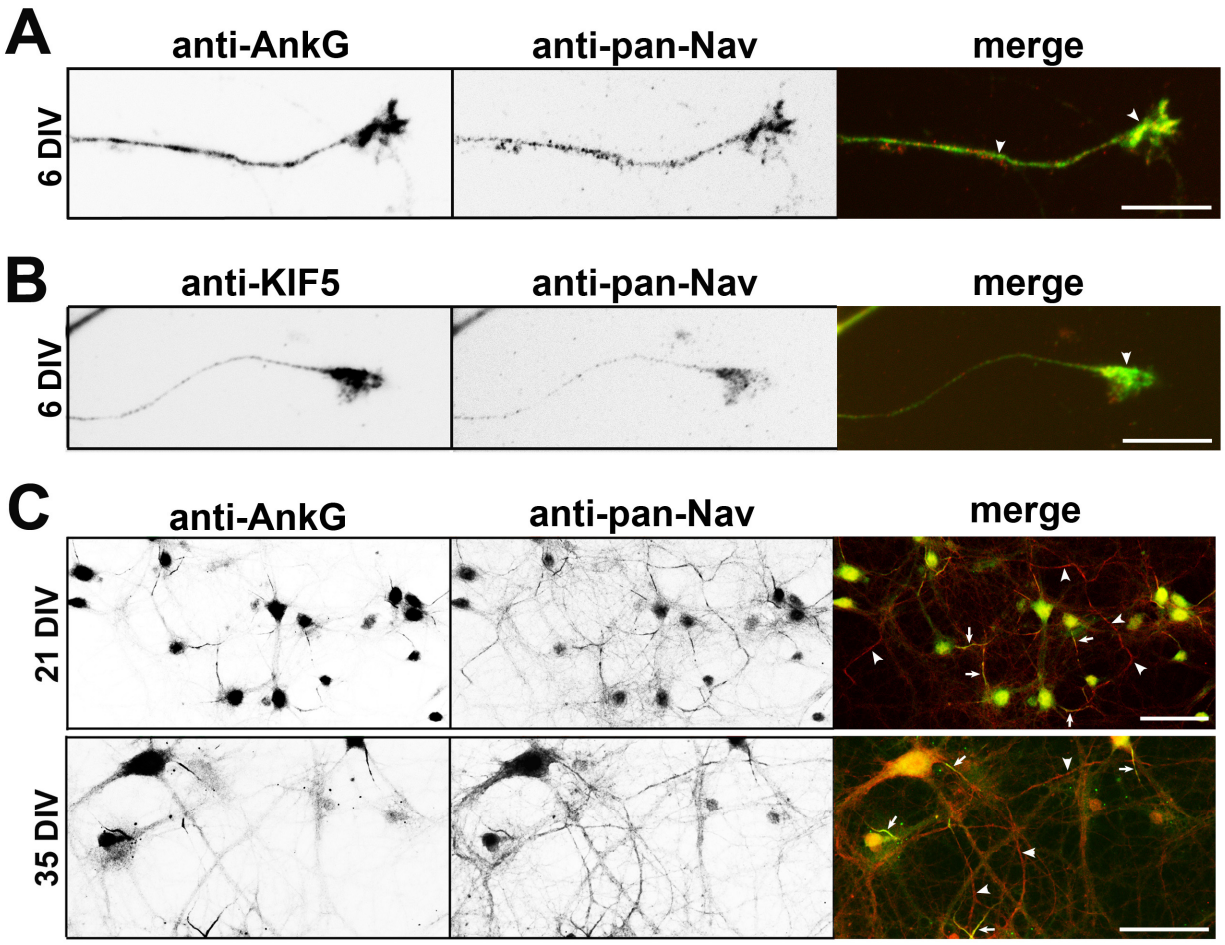

Figure S1. Development-dependent colocalization of AnkG, KIF5 and Nav channels.
Related to Figure 1.
A, AnkG and Nav channels colocalize in distal axons and growth cones in hippocampal neurons at 6 DIV. Signals are inverted in gray scale images. In the merged image: AnkG in green and Nav in red. **B,** KIF5 and Nav channels colocalized in distal axons and growth cones in hippocampal neurons at 6 DIV. In the merged image: KIF5 in green and Nav in red. **C,** In mature neurons, AnkG and Nav channels colocalized at the AIS, while Nav channels also localized into distal axons of neurons at 21 DIV (top) and 35 DIV (bottom). In merged images: AnkG in green and Nav in red. Arrows, proximal axons; Arrowheads, distal axons. Scale bars, 20 μm in **A** and **B**, 100 μm in **C**.

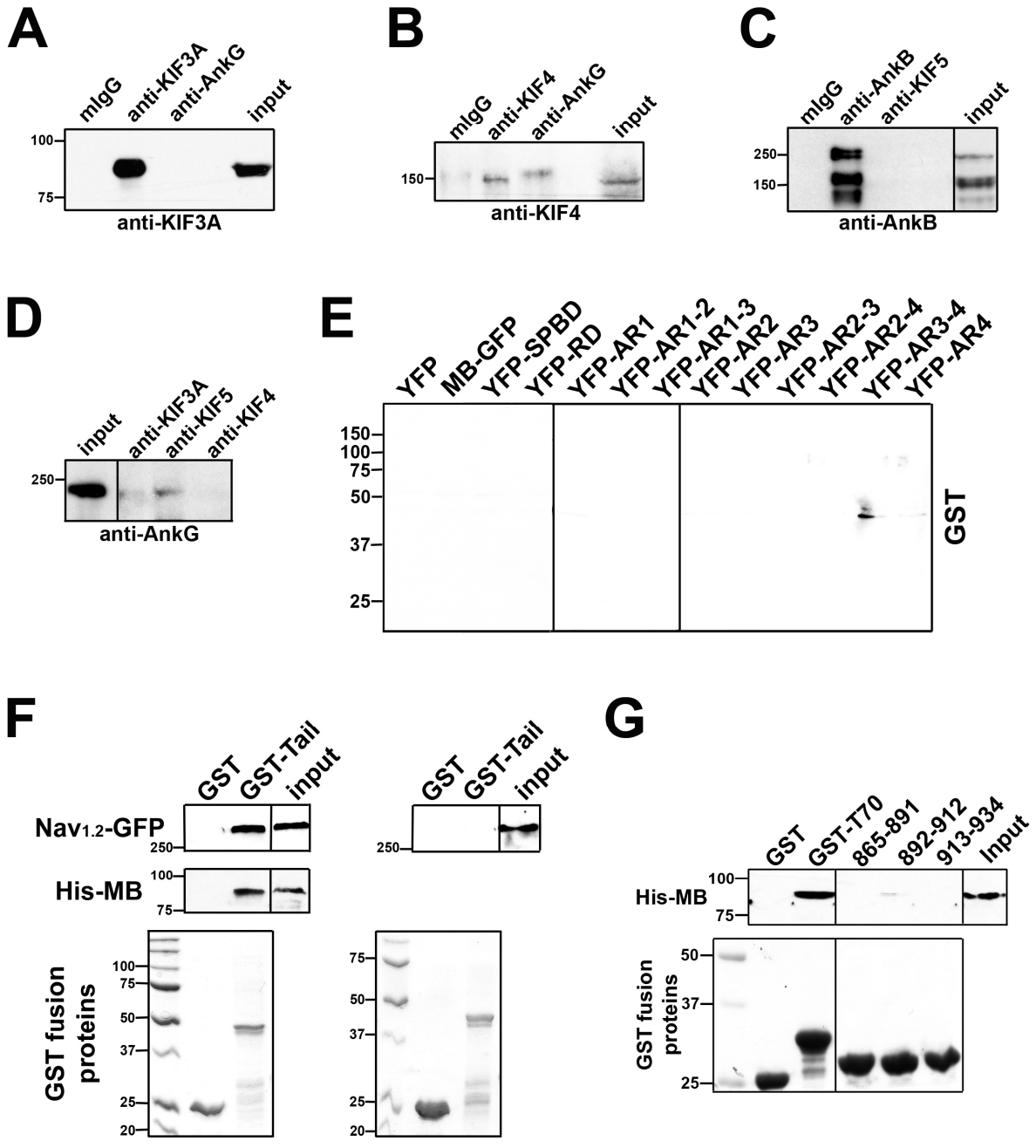

Figure S2. Protein binding assays to determine the interaction of AnkG, $Nav_{1.2}$ and KIF5B. Related to Figure 2.

A, AnkG antibody did not pull down KIF3A from brain lysates of mouse pups (postnatal day 7 to 21). 10% of KIF3A pulldown was loaded; 5% was loaded for both inputs. The same conditions were used from **B** to **D**. **B,** Pulldown experiment of KIF4 by the AnkG antibody. The faint band above the KIF4 bands is most likely a nonspecific band. **C,** AnkB antibody did not pull down KIF5. Despite that AnkG and AnkB have conserved N-terminal ankyrin repeats, their C-terminal regions differ, which interferes with the binding. **D,** The antibody of KIF5, but not KIF3A and KIF4, pulled down AnkG. The pull down was not efficient, which may result from the very large size of AnkG and many other binding proteins. The very faint signal in the KIF3A-pulldown lane is likely a non-specific band due to its smaller size.

Even if it were a real band, it does not affect the conclusion. **A-D** show the control experiments for Figure 2A. **E,** YFP fused AnkG fragments were not pulled down by purified GST. The anti-GFP antibody was used for the Western blotting. This is the control experiment for Figure 2C. **F,** GST-Tail pulled down Nav1.2-GFP full length protein in the presence of His-MB. Glutathione beads (30 μl) coated with GST or GST-Tail were incubated with (left) or without (right) purified His-MB (4 μg), and further incubated with 1 ml HEK293 cell lysates containing expressed $Nav_{1.2}$-GFP. Colloidal blue was used to stain GST fusion proteins (bottom). The anti-6×His (middle) and anti-GFP (top) antibodies were used for Western blotting. **G,** Three fragments within the T70 region, GST-$Tail_{865-891}$, GST-$Tail_{892-912}$ and GST-$Tail_{913-934}$, failed to efficiently pull down His-MB. Colloidal blue was used to stain GST fusion proteins (bottom). The anti-6×His antibody was used for Western blotting (top). Each pulldown assay was performed at least three times.

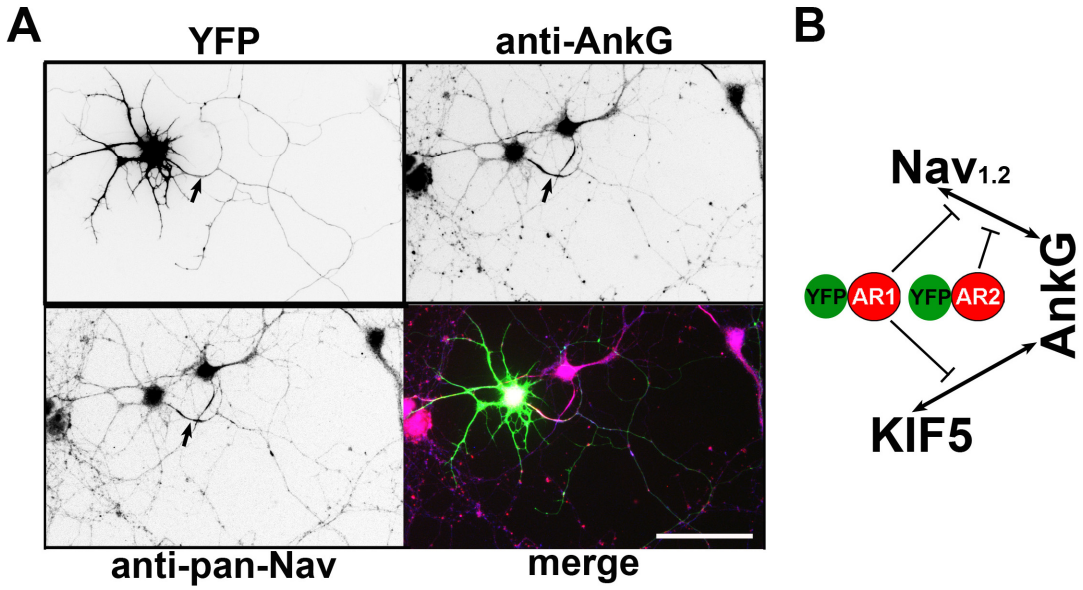
A
YFP
anti-AnkG
anti-pan-Nav
merge
B
Nav1.2
YFP
AR1
YFP
AR2
AnkG
KIF5

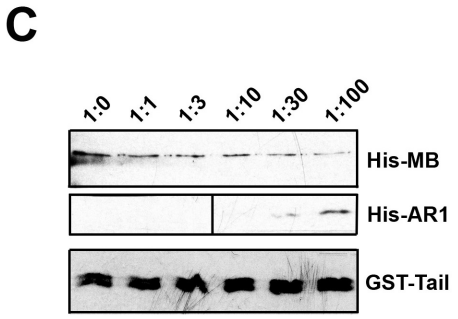
C
1:0
1:1
1:3
1:10
1:30
1:100
His-MB
His-AR1
GST-Tail

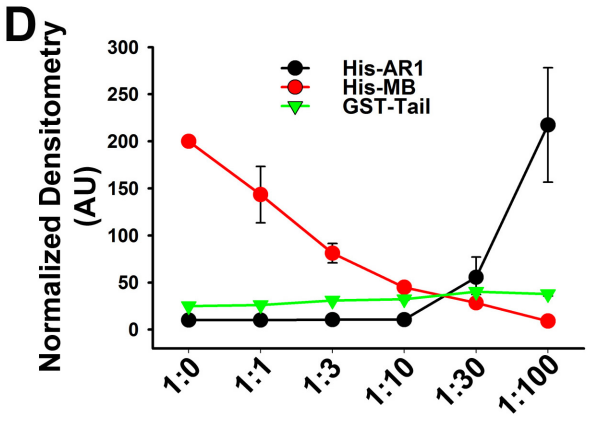
D
Normalized Densitometry (AU)
300
250
200
150
100
50
0
His-AR1
His-MB
GST-Tail
1:0
1:1
1:3
1:10
1:30
1:100

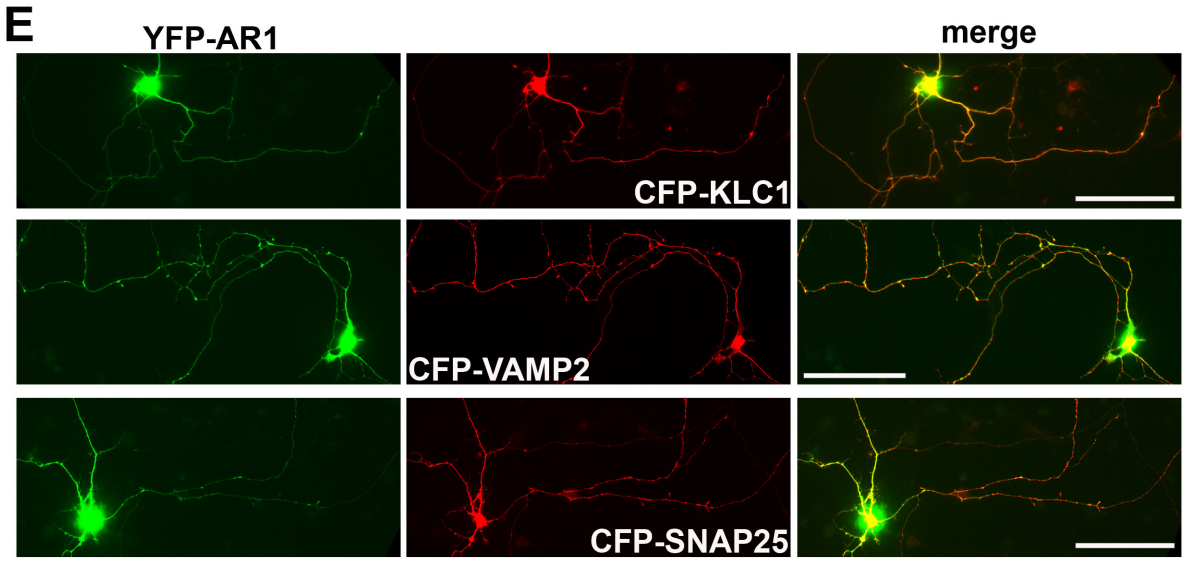
E
YFP-AR1
merge
CFP-KLC1
CFP-VAMP2
CFP-SNAP25

Figure S3. Disrupting AnkG-KIF5B binding by using YFP-AR1 and YFP-AR2, dominant-negative fragments from AnkG.

Related to Figure 3.

A, Endogenous AnkG and Nav channels in a YFP-transfected neuron. Hippocampal neurons were transfected at 12 DIV, fixed and stained at 17 DIV. In single images, signals are inverted. Black arrows, proximal axons. **B,** Diagram of the dominant-negative actions of YFP-AR1 and YFP-AR2. **C,** His-AR1 competed with His-MB for binding to GST-Tail. GST-Tail (1.7 μg) was first coated on glutathione beads and further used to pull down purified His-MB (2.8 μg, so that GST-Tail and His-KLC1 are in a 1:1 molar ratio) mixed with different amount of His-AR1. Molar ratios between His-MB and His-AR1 used were 1:0, 1:1, 1:3, 1:10, 1:30 and 1:100. An anti-His antibody was used to detect His-MB and His-AR1 (top two panels). An anti-GST antibody was used to detect GST-Tail (bottom). **D,** The densitometry result for **C**. Bands of His-AR1 are normalized with the strongest band in the last lane (1:100). His-MB bands are normalized using the first lane (1:0). GST-Tail bands are normalized using the first lane (1:0). **E,** Expression of YFP-AR1 (green) did not reduce the axonal levels of CFP-KLC1, CFP-VAMP2 and CFP-SNAP25. Hippocampal neurons were co-transfected at 5 DIV and fixed at 8 DIV. Scale bars, 100 μm.

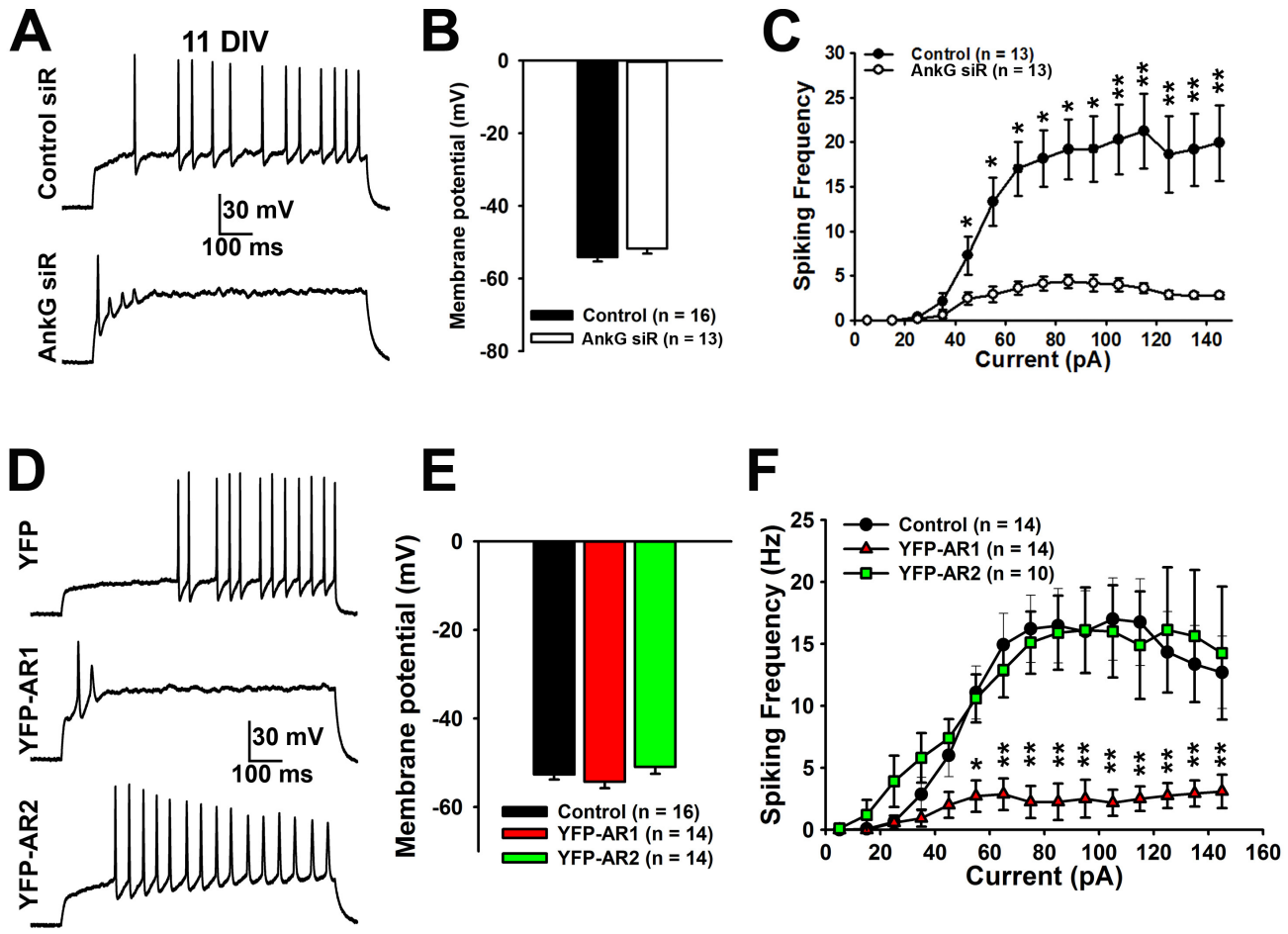

Figure S4. Knockdown of AnkG using siRNA or over-expression of YFP-AR1 altered the action potential firing.

Related to Figure 4.

A, AnkG siRNA but not control siRNA markedly reduced the action potential (AP) firing frequency, revealed by current clamp recording. In this experiment, hippocampal neurons were transfected with siRNA constructs at 5 DIV and recorded at 11 DIV. A square current pulse (1000 ms and 55 pA) was injected into the soma of the neuron to induce APs. **B,** There was no change in the resting membrane potential. **C,** The input-output relationship was markedly reduced by AnkG siRNA. 1000-ms duration currents of increasing amplitude (from 5 to 145 pA with increments of 10 pA) were injected into the soma to induce APs. t-test: *, $p < 0.01$; **, $p < 0.001$. D, **D-F,** YFP-AR1, but not YFP or YFP-AR2 markedly reduced spiking frequency (Hz). Hippocampal neurons were transfected at 5 DIV and recorded at 7-8 DIV. **D,** APs induced by square-pulse injections (1000 ms, 80 pA). **E,** The resting membrane potential did not change. **F,** The input-output relationship was markedly altered in YFP-AR1-expressing neurons. 1000-ms duration currents of increasing amplitude (from 5 to 145 pA with increments of 10 pA) were injected into the soma to induce APs. One way ANOVA followed by Dunnett's test. *, $p < 0.01$; **, $p < 0.001$.

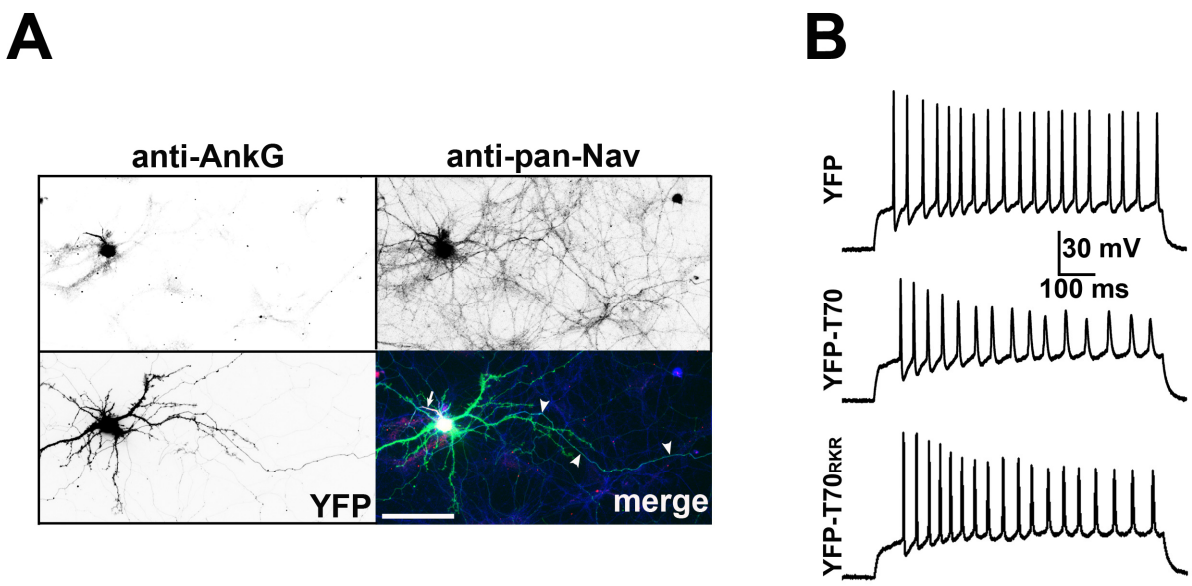

Figure S5. YFP-T70, but not YFP or YFP-T70$_{RKR}$, decreased AP firing.
Related to Figure 5.
A, YFP-expressing neuron (green in merged) was stained for endogenous AnkG (red in merged) and Nav channels (blue in merged). Hippocampal neurons were transfected at 12 DIV, fixed and stained at 17 DIV. In single images, signals are inverted. White arrow, the AIS; White arrowheads, middle and distal axons. Scale bars, 100 μm. **B,** In the presence of YFP-T70, AP firing reduced. APs induced by square-pulse injection (1000 ms, 80 pA).

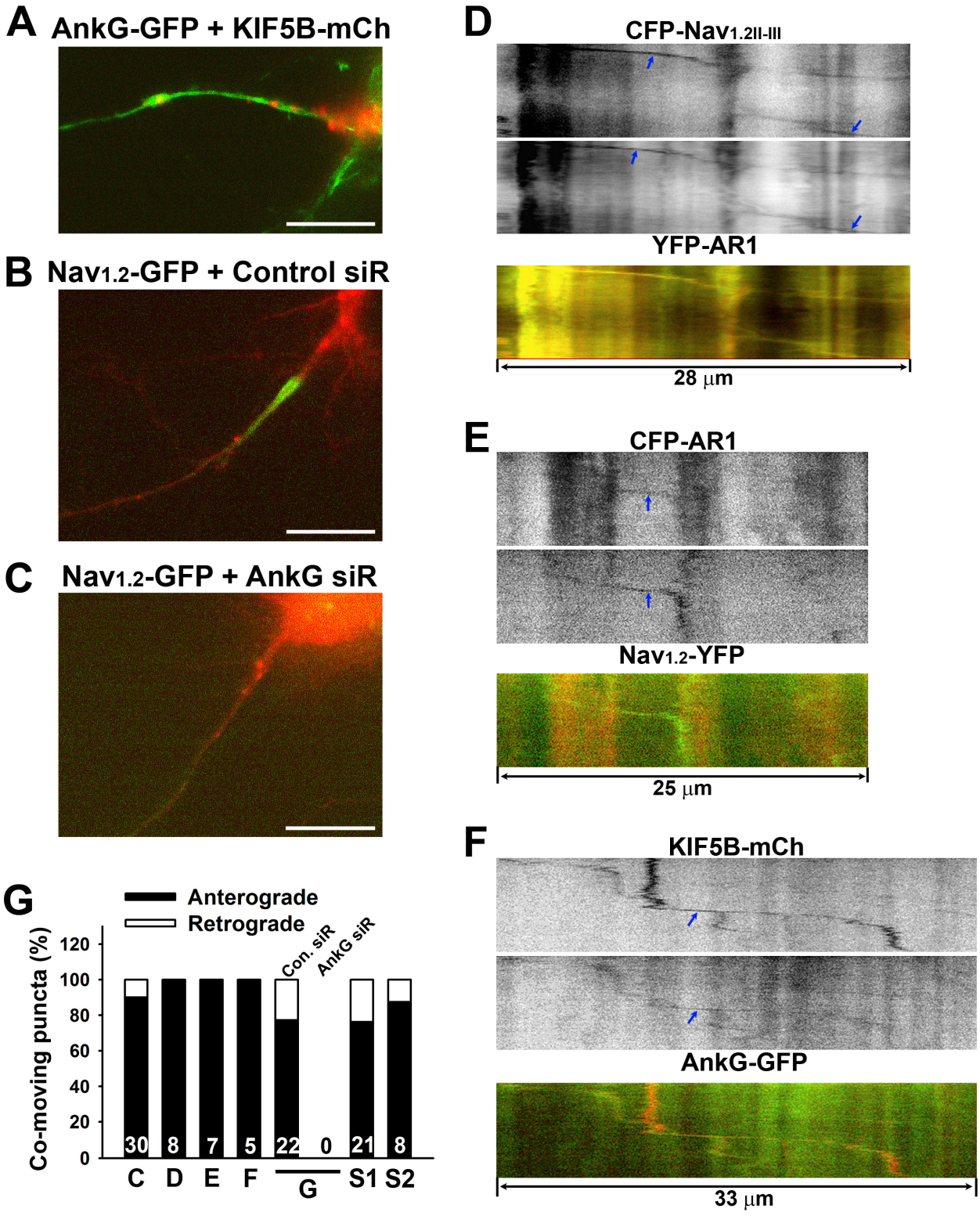

Figure S6. Live-cell imaging of AnkG-GFP, $Nav_{1.2}$-GFP and KIF5-mCh.
Related to Figure 6.

Hippocampal neurons were transfected at 5 DIV and imaged with 100x oil lens 2-5 days later. Neuronal somas are on the right side. **A,** Co-expression of AnkG-GFP (green) and KIF5B-mCh (red) along proximal axons. **B,** $Nav_{1.2}$-GFP (green) was clustered at the axon initial segment in the presence of control siRNA (red; mCherry was expressed in the siRNA plasmid). **C,** The axonal level of $Nav_{1.2}$-GFP (green) markedly decreased in the presence of AnkG siRNA (red). Scale bars, 40 μm. **D,** Kymograph of anterograde co-transport of YFP-AR1 (green in merged) and CFP-$Nav_{1.2II-III}$ (red in merged). Signals are inverted in gray scale images. Blue arrows, anterograde co-moving puncta. **E,** Kymograph of anterograde co-transport of $Nav_{1.2}$-YFP (green in merged) and CFP-AR1 (red in merged). **F,** Kymograph of anterograde co-transport of AnkG-GFP (green in merged) and KIF5B-mCh (red in merged), preincubated with 2.5 μM Latrunculin A at 37°C for 2 hrs. **G,** Percentage of anterograde and retrograde co-moving puncta (C: CFP-AR1 + KIF5B-YFP; D: MB-GFP + KIF5B-mCh; E: AnkG-GFP + KIF5B-mCh; F: $Nav_{1.2}$-GFP + KIF5B-mCh; G: CFP-$Nav_{1.2II-III}$ + KIF5B-YFP; S1: CFP-$Nav_{1.2II-III}$ + YFP-AR1; S2: CFP-AR1 + $Nav_{1.2}$-YFP). The number of co-moving puncta is provided for each bar. The time length was 198 sec for all kymographs and the distance is provided for each one.

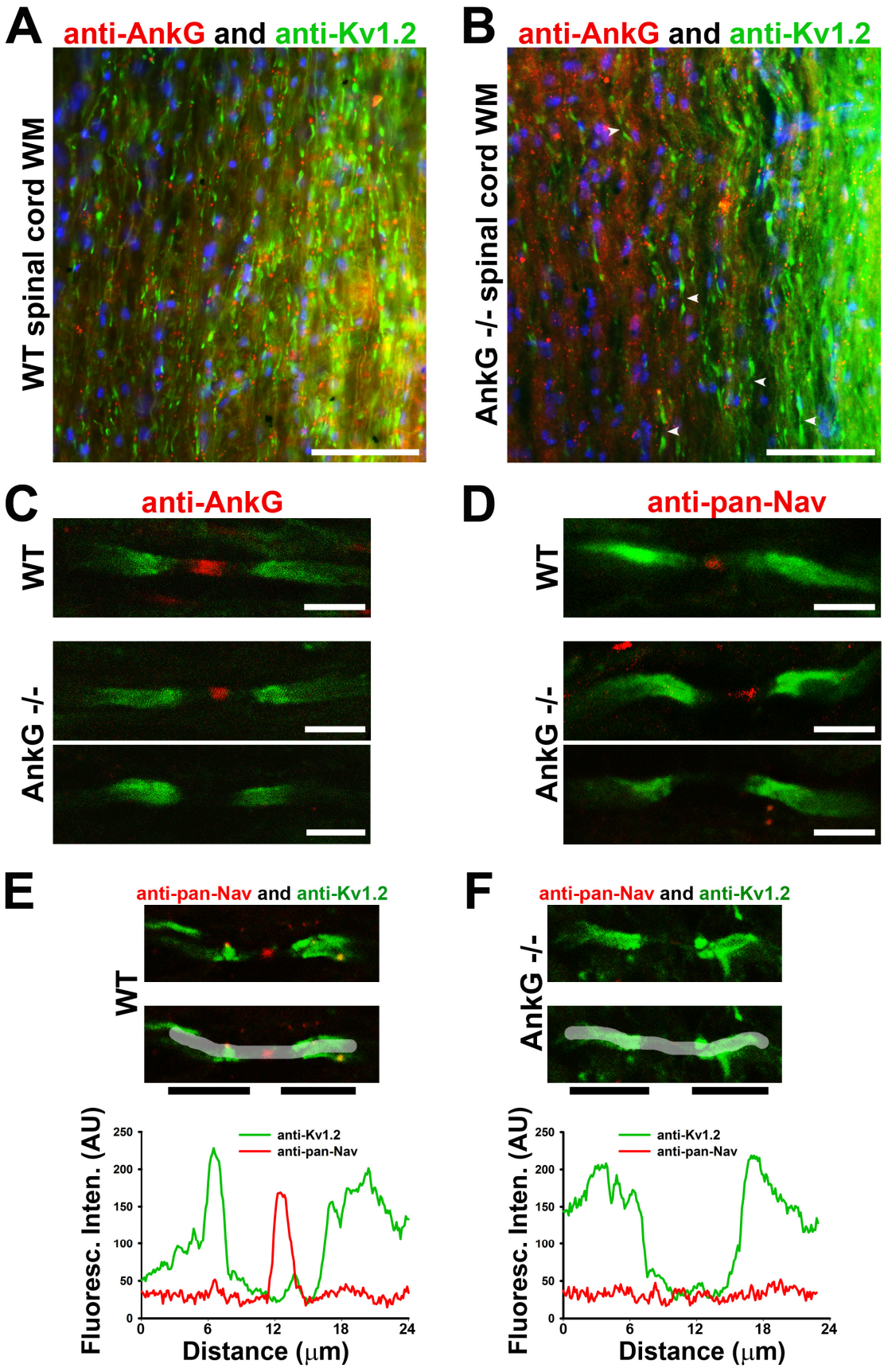
A
anti-AnkG and anti-Kv1.2
WT spinal cord WM
B
anti-AnkG and anti-Kv1.2
AnkG -/- spinal cord WM
C
anti-AnkG
WT
AnkG -/-
D
anti-pan-Nav
WT
AnkG -/-
E
anti-pan-Nav and anti-Kv1.2
WT
anti-Kv1.2
anti-pan-Nav
Fluoresc. Inten. (AU)
Distance (μm)
F
anti-pan-Nav and anti-Kv1.2
AnkG -/-
anti-Kv1.2
anti-pan-Nav
Fluoresc. Inten. (AU)
Distance (μm)

Figure S7. AnkG, Nav and Kv1.2 staining along myelinated axons.

Related to Figure 7.

A and **B**, low magnification images show Kv1.2 (green) and AnkG (red) were clustered in the nodal and JXP regions of myelinated axons, respectively, in the white matter of spinal cord of WT (**A**) and AnkG -/- (**B**) mice. Arrowheads, the nodal regions missing AnkG staining. **C**, high magnification images show AnkG was clustered (red) at the node of a WT myelinated axon (top), but disappeared from the nodal region of some axons in SCWM of AnkG -/- mice (bottom). **D**, Nav channels were clustered (red) at the node of a WT myelinated axon (top), but disappeared from the nodal region of some axons in SCWM of AnkG -/- mice (bottom). Scale bars, 100 μm in **A** and **B**, 10 μm in **C** and **D**.

E, Quantification of pan-Nav (red) and Kv1.2 (green) fluorescence intensities along a myelinated axonal segment from WT cerebellum (top). Average intensities along a line at the center of the axon in 5 to 10 pixels width (middle) are plotted at the bottom. **F,** Quantification along a myelinated axonal segment from AnkG -/- cerebellum (top). Average intensities along the axon are plotted at the bottom. Black bars under the images indicate the regions for calculating the basal level of pan-Nav channel signals, in which the nodal region is not included. There is no significant difference in basal level ($F_{Nav}/F_{Kv1.2}$, WT: 0.12 ± 0.01 (n = 25); AnkG -/-: 0.10 ± 0.01 (n = 32)). However, there is significant difference when the nodal region is included ($F_{Nav}/F_{Kv1.2}$, WT: 0.22 ± 0.01 (n = 25); AnkG -/-: 0.10 ± 0.01 (n = 32); unpaired t-test, $p < 0.01$). The pairs of JXP Kv1.2 clusters flanking the nodes were not always perfectly symmetric because many axons were not perfectly resting on the focal plane of imaging.

Supplemental Experimental Procedures

Antibodies and immunocytochemistry

Antibodies used include the following: mouse monoclonal anti-green fluorescent protein (GFP), anti-AnkG, anti-Kv1.2, anti-6×His, and anti-AnkB antibodies (NeuroMab UC Davis clone N86/8, N106/36, K14/16, N144/14, and N105/13 respectively), rabbit anti-microtubule-associated protein 2 (MAP2) and rabbit anti-pan-Nav channels (Millipore, Billerica, MA, USA), mouse anti-kinesin heavy chain (KIF5) H2, anti-pan-Nav channel and anti-KIF4 antibodies (Sigma-Aldrich, St Louis, MO, USA), Rabbit anti-KIF3A antibody (Abcam, Cambridge, MA, USA), Cy2-, Cy3-, and Cy5-conjugated secondary antibodies (Jackson ImmunoResearch Laboratories, West Grove, PA, USA). The procedures of immunocytochemistry were described previously (Gu et al., 2006; Xu et al., 2007). In brief, the neurons were fixed with 4% formaldehyde (from 10% ultrapure EM grade and methanol free; Polysciences, Warrington, PA) and 4% sucrose in PBS for 20 min, and stained with specified antibodies under permeabilized conditions (in the presence of 0.2% Triton X-100) to label total proteins.

Immunoprecipitation and Western blotting

Mouse brains were homogenized with Dounce tissue grinder in immunoprecipitation (IP) buffer (50 mM Tris-Cl, pH 7.4, 150 mM NaCl, 1% Triton X-100, and a Complete protease inhibitor tablet) then solubilized for 2 h at 4°C, and centrifuged at 50,000 *g* for 30 min at 4°C. The supernatant (1 ml for each condition) was incubated (2–4 h, 4°C) with 2 µl of rabbit anti-pan-Nav, 4 µl of mouse anti-KIF5 H2, anti-AnkG antibodies, or control mouse IgG, and 50 µl of protein G (or A)-agarose beads (Roche, Indianapolis, IN, USA). The beads were washed six times with the IP buffer and eluted with 2× sample buffer. The immunoprecipitants were resolved by SDS-PAGE, transferred to a polyvinylidene difluoride (PVDF) membrane, and subjected to Western blotting with either the H2 or anti-pan-Nav channel antibody (1:1000 dilution).

Protein purification and in vitro binding assay

Expression of GST- or 6×His-tagged fusion proteins was induced in BL21 *Escherichia coli* cells with 1 mM IPTG (isopropyl β-D-thiogalactoside) for 4 h at 37°C. Bacterial pellets were solubilized with sonication in the IP buffer at 4°C, and centrifuged at 50,000 *g* for 30 min at 4°C. The supernatants were incubated either with glutathione beads (GE Healthcare Bio-Sciences, Sweden) or with Co^{2+} beads (Clontech Laboratories, Inc, Mountain View, CA, USA) at 4°C for 3 h. After extensive washing, the beads coated with purified fusion proteins were eluted with the IP buffer containing either 20 mM glutathione or 150 mM imidazole. The elution was further dialyzed with the IP buffer at 4°C overnight. In *in vitro* binding assays in Fig. 2E, purified GST fusion protein (2 µg) were incubated with glutathione beads in IP buffer at 4°C for 1 h, washed 6 times in IP buffer, then His-MB (2 µg) was incubated at 4°C for 2 h, washed 6 times in IP buffer, and then eluted with 2× sample buffer.

In the experiment of mapping KIF5-binding site in AnkG in Fig. 2C, glutathione beads coated with GST fusion proteins were further incubated with the supernatant from HEK293 cells expressing yellow fluorescent protein (YFP) fusion proteins. The precipitants were eluted with 2× sample buffer, resolved in SDS-PAGE, and then subjected to Western blotting and Colloidal Blue staining. Each immunoprecipitation or pulldown assay was performed at least three times.

Hippocampal neuron cultures and transfection

Hippocampal neuron culture was prepared as previously described from embryonic day 18 (E18) embryos (Gu et al., 2006). In brief, 2 d after neuron plating, 1 µM cytosine arabinose (Sigma-Aldrich) was added to the neuronal culture medium to inhibit glial growth for the subsequent 2 d, and then replaced with the normal culture medium. The culture medium was replenished twice a week by replacing one-half of the volume. For transient transfection, neurons in culture from 5 to 10 DIV (days *in vitro*) were incubated in Opti-MEM containing 0.8 µg of cDNA plasmid and 1.5 µl of Lipofectamine 2000 (Invitrogen, Carlsbad, CA, USA) for 20 min at 37°C. Neurons in culture from 11 to 21 DIV were transfected with the Ca^{2+}/phosphate method (Jiang and Chen, 2006) with some modification. In brief

tube A (1 µg cDNA, 3.1 µl 2M $CaCl_2$, up to 25 µl ddH_2O) was added to 25 µl 2× HBS (136.9 mM NaCl, 1.5 mM $Na_2PO_4 \cdot 7H_2O$, 26 mM HEPES, pH 7.05) in tube B and incubated at room temperature (RT). for 15-20 min. Then 0.5 ml medium was removed from 1 well of 24 well plate and placed in 15 ml conical. 20-30% maintenance media (of 0.5 ml) were added to conical and equilibrated at 37°C 10% CO_2 for 15 min. A+B mixture was added to well and incubated for 1 h at 37°C in 5% CO_2. Media were removed and then replaced with the 10% CO_2 equilibrated buffer. Expression was checked the next day.

Short interfering RNA knockdown of endogenous AnkG

Construction and validation of vector-based short interfering RNA (siRNA) strategy to suppress the levels of endogenous proteins in rat hippocampal neurons were previously described (Xu et al., 2007). We used the previously generated AnkG siRNA construct made from insertion of a sense and antisense loop of AnkG (21 nucleotides) into pRNAT-H1.1/neo vector (GenScript, Piscataway, NJ, USA). The GFP coding region in the vector was replaced with the coding sequence for mCherry between BamH1 and HindIII sites (Gu and Gu, 2010). Therefore, the neurons transfected with the siRNA plasmid expressed mCherry as the indicator for transfection. The siRNA plasmid was transfected into neurons at 5 DIV and fixed and stained at 21 DIV.

Fluorescence microscopy and quantification

Fluorescence images were captured with a Spot CCD camera RT slider (Diagnostic Instrument Inc., Sterling Heights, MI, USA) in a Zeiss upright microscope, Axiophot, using Plan Apo objectives 20×/0.75 and 100×/1.4 oil, saved as 16 bit TIFF files, and analyzed with NIH ImageJ and SigmaPlot 12.0 for fluorescence intensity quantification. Exposure times were controlled so that the pixel intensities in dendrites and axons were below saturation, but the same exposure time was used within each group of an experiment. Only transfected neurons with clearly separated dendrites and axons, and isolated from other transfected cells, were chosen for analysis. The measurement of fluorescence intensities along axons was previously described (Gu et al., 2006; Xu et al., 2007; Xu et al., 2010).

Whole-cell patch-clamp recording

The internal solution and Hank's buffer were previously described for recording of primary cultured neurons (Gu et al., 2012). Hank's buffer: 150 mM NaCl, 4 mM KCl, 1.2 mM $MgCl_2$, 10 mg/ml glucose, 1 mM $CaCl_2$, 20 mM HEPES (pH 7.4). The internal solution of electrical pipettes: (in mM) 122 $KMeSO_4$, 20 NaCl, 5 Mg-ATP, 0.3 GTP and 10 HEPES (pH 7.2). Both current clamp and voltage clamp recording procedures were previous described (Gu et al., 2012).

Two-color live-cell imaging

Both the procedure and quantification of two-color live-cell imaging were previously described (Barry, 2013; Gu and Gu, 2010; Xu et al., 2010). In brief, neurons growing on 25 mm coverslips were loaded into the imaging chamber (Molecular Devices, Downingtown, PA, USA) and incubated with imaging buffer (HE-LF medium (Brainbits, Springfield, IL, USA) plus 2% B-27, 0.5 mM Glutamine, and 25 µM Glutamate) at RT. The timelapse imaging setup was built upon a Nikon (Nikon Inc., Melville, NY, USA) TE2000 inverted microscope. Images were captured with a CCD camera Coolsnap HQ (Photometrics, Tucson, AZ, USA) through CFP or YFP filter sets with 1 second exposure time. The filters were changed through filter wheels controlled through Lambda 10-3 (Sutter Instrument, Novato, CA, USA) by MetaMorph software (Molecular Devices). The time-lapse imaging was performed with 2-second interval for 100 frames. All measurements were carried out on kymographs made with the MetaMorph program as previous described (Gu and Gu, 2010). The total time for each movie is 198 sec. Our quantification only included puncta that moved 4 µm or further. We calculated the transport velocity using kymograph. We calculated the frequency of transport events (or the average number of moving puncta per movie) F(#/min) = n / (198 sec / 60 sec/min). For instance, if one moving punctum (n = 1) is observed in one movie (total 3.3 minute long), F equals 0.3. F equals 0 if no moving punctum was seen in a movie. F equals 0.6 or 0.9 if 2 or 3 moving puncta were seen, respectively. Anterograde and retrograde puncta were presented as "+" and "-" values.

AnkG KO mice, cardiac perfusion, tissue fixation and sectioning

AnkG KO mice were previously published (Jenkins and Bennett, 2001). The procedure of cardiac perfusion, tissue fixation and sectioning were previously described (Jukkola et al, 2012). In brief, animals were deeply anesthetized with 250 mg/kg avertin (12.5 mg/mL 2,2,2-tribromoethanol dissolved in ddH_20/0.025% 2-methyl-2butanol) (Sigma-Aldrich). The thoracic cavity was opened to expose the heart, and the mice were perfused with 20-30 ml ice-cold PBS followed by 20 ml 4% formaldehyde in PBS. The brain and spinal cord were carefully removed and post-fixed for 1 hr in 4% formaldehyde in PBS. The brain was cut into 3-mm blocks using an acrylic brain matrix (Braintree Scientific, Braintree, MA, USA) and placed in 30% sucrose for at least 24 hr before sectioning. Brain and spinal cord tissues were arranged in the same block, embedded in optimal cutting temperature (OCT) media (Sakura Finetek USA, Inc., Torrance, CA, USA), and stored at -80 °C until sectioning. The spinal cord was cut into segments and arranged for both transverse and longitudinal sectioning. The tissue blocks were cut with a Microm HM550 cryostat (Thermo Scientific, Waltham, MA, USA) and the 40-µm sections were collected on Superfrost Plus microscope slides (FisherScientific, Pittsburgh, PA, USA) for storage at -20°C.

Immunofluorescent staining of sections of brain and spinal cord

Sections were incubated in PBS/0.3% Triton X-100 for 1 h at RT to permeabilize the tissue, then blocked with 2.5% normal goat or donkey serum (matched with the host species of the secondary antibody) for 1 h at RT. The primary antibodies were then added in blocking solution, and the sections were incubated for 3 h at RT, then overnight at 4°C. The next day, the sections were rinsed 10 × 5 min at RT, the appropriate secondary antibody was added in blocking solution, and the sections were incubated for 3 h at RT. Then, the sections were incubated in Hoechst 33342 for 10 min at RT. Sections were rinsed 10 × 5 min and coverslipped using tris-buffered Fluoro-Gel mounting media (Electron Microscopy Sciences, Hatfield, PA, USA).

Confocal microscopy

High-magnification confocal images were captured with a Leica TCS SL confocal imaging system (Leica Microsystems, Mannheim, Germany), using a 100× HCX Plan Apo CS oil immersion objective (numerical aperture = 1.40). Multiple channels were acquired simultaneously, and the signal was averaged over six scans. Channel crosstalk was eliminated through optimization of the laser line intensity by acousto-optical tunable excitation filters, and by spectral detectors allowing precisely-defined bandwidth adjustment. Images were saved as 8-bit TIFF files and adjusted for brightness and contrast using Adobe Photoshop 7.0.

Surgeries and microinjection of viral vectors

YFP, YFP-T70, or YFP-$T70_{RKR}$ was overexpressed in mouse cerebellum by stereotaxic injection of recombinant AAV2 virus. Each mouse was unilaterally injected on the right side, leaving the uninjected left side a within-subject control. Cohorts of mice injected with AAV-YFP (n = 6), AAV-YFP-T70 (n = 6), or AAV-YFP-$T70_{RKR}$ (n = 6) were produced for between-subject comparisons.

The stereotaxic injection setup consisted of a Hamilton syringe and tubing system, primed with water and connected to a 33 gauge injector cannula (Plastics One, Roanoke, VA, USA). The injection was monitored visually by checking the movement of a small air bubble within a glass capillary. The viral vector was backfilled into the injector, downstream of this air bubble before the surgery.

The mice were anesthetized with a mixture of 100 mg/kg ketamine and 15 mg/kg xylazine (Sigma-Aldrich). Using aseptic surgical procedures, the mice were then fixed into a stereotaxic frame (Stoelting Co., Wood Dale, IL, USA) and a small skin incision was made over the skull. The skull was made level, and the location of the Bregma landmark was recorded. A small burr hole was made over the regions using a Dremel tool. An injection needle was inserted and the viral vector (0.75 µl undiluted total volume) were administered to the cerebellum (Anterior/Posterior, -5.8; Medial/Lateral, ±1.5; Dorsal/Ventral -2.5 & -1.5 relative to Bregma in mm) at a rate of 0.25 µl/min using a syringe

pump. The mice were then sutured and administered post-operative care for one week. Mouse cerebellum was fixed and sectioned 2 to 3 weeks after injection for immunohistochemistry studies.

Supplemental References

Barry, J., Xu, M., Gu, Y., Dangel, W., Jukkola, P., Shrestha, C., and Gu, C. (2013). Activation of conventional kinesin motors in clusters by Shaw voltage-gated potassium channels. J Cell Sci *126*, 2027-2014.

Gu, C., Zhou, W., Puthenveedu, M.A., Xu, M., Jan, Y.N., and Jan, L.Y. (2006). The microtubule plus-end tracking protein EB1 is required for Kv1 voltage-gated K^+ channel axonal targeting. Neuron *52*, 803-816.

Gu, Y., Barry, J., McDougel, R., Terman, D., and Gu, C. (2012). Alternative splicing regulates Kv3.1 polarized targeting to adjust maximal spiking frequency. J Biol Chem *287*, 1755-1769.

Gu, Y., and Gu, C. (2010). Dynamics of Kv1 channel transport in axons. PLoS One *5*, e11931.

Jenkins, S.M., and Bennett, V. (2001). Ankyrin-G coordinates assembly of the spectrin-based membrane skeleton, voltage-gated sodium channels, and L1 CAMs at Purkinje neuron initial segments. J Cell Biol *155*, 739-746.

Jiang, M., and Chen, G. (2006). High Ca^{2+}-phosphate transfection efficiency in low-density neuronal cultures. Nat Protocols *1*, 695-700.

Jukkola, P., Lovett-Racke, A., Zamvil, S., Gu, C. (2012). Alterations of K^+ channels in the progression of EAE. Neurobiol Dis *47*, 280-293.

Xu, M., Cao, R., Xiao, R., Zhu, M.X., and Gu, C. (2007). The axon-dendrite targeting of Kv3 (Shaw) channels is determined by a targeting motif that associates with the T1 domain and ankyrin G. J Neurosci *27*, 14158-14170.

Xu, M., Gu, Y., Barry, J., and Gu, C. (2010). Kinesin I transports tetramerized Kv3 channels through the axon initial segment via direct binding. J Neurosci *30*, 15987-16001.